

## SEISMIC HAZARD MAPS FOR THE FRENCH METROPOLITAN TERRITORY

Stéphane DROUET<sup>1</sup>, Kristell LE DORTZ<sup>1</sup>, Ramon SECANELL<sup>1</sup>, Gabriele AMERI<sup>1</sup>, Gloria SENFAUTE<sup>2</sup>, Nicolas HUMBERT<sup>3</sup>

### ABSTRACT

The undergoing study aims at the elaboration of a probabilistic seismic hazard maps for metropolitan France taking into account the outcomes of recent research projects such as SIGMA (Research on Seismic Ground Motion Assessment, 2011 – 2016), which was devoted to improve knowledge on data, methods and tools to better quantify uncertainties in seismic hazard estimates. A new earthquake catalogue for France was developed including a revision of magnitude and depth for historical events and of location and magnitude for instrumental events. This catalogue is used as the backbone catalogue for the present study. Three area source models developed independently by 3 institutions are considered for which seismic activity is characterized using the Gutenberg-Richter model including an exploration of earthquake location and magnitude uncertainty. In addition, a zoneless approach is considered using spatially-adaptive kernel functions. The concept of large seismotectonic domains is introduced in order to constrain the estimation of the Gutenberg-Richter b-value and to derive maximum magnitude distributions using the Bayesian approach. The ground-motion model includes two GMPEs developed specifically for France as well as two additional models. Tests were carried on in order to investigate if the adopted ground-motion characterization logic tree captures epistemic uncertainty. Uncertainties related to the seismic activity (parameters a and b of the Gutenberg-Richter models), maximum magnitude, and hypocentral depth is also explored. The objective of this study is to produce probabilistic hazard maps for a grid with a spatial sampling of 10 km for two return periods (475 and 2475 years) and three spectral periods (PGA, 0.2 and 1.0 seconds).

*Keywords: Seismic hazard; Uncertainties; France*

### 1 INTRODUCTION

Probabilistic seismic hazard (PSH) assessment is used for quantifying the seismic hazard on a site or on a grid of sites. For regions of low to moderate seismicity such as metropolitan France PSH assessment is a significant challenge requiring accurate evaluation and appropriate treatment of uncertainties.

The last seismic hazard maps produced for France were published about 15 years ago and significant improvements in seismic hazard assessment have been made since then. In particular, the SIGMA project aimed at a better understanding and characterization of all uncertainties (Pecker et al 2017). During this project (2011 – 2016) several results with operational applications have been obtained (Martin et al., 2017): homogenous seismic catalogue in Mw for France, seismic ground-motion database (RESORCE) to develop Ground Motion Prediction Equations for Europe and specific models for France, best practices guideline for site characterization and operational guide to account for site effects.

The present study, which is the first step of a long term project, makes use of these SIGMA outcomes to elaborate a probabilistic seismic hazard maps for the French metropolitan territory. The objective is

---

<sup>1</sup>GEOTER, Auriol, France, [s.drouet@fugro.com](mailto:s.drouet@fugro.com)

<sup>2</sup>EDF/Lab, Saclay, France, [gloria.senfaute@edf.fr](mailto:gloria.senfaute@edf.fr)

<sup>3</sup>EDF, France, [nicolas.humbert@edf.fr](mailto:nicolas.humbert@edf.fr)

to produce seismic hazard maps for 475 and 2475 years return period at 3 spectral periods (100 Hz ~PGA, 5 Hz and 1 Hz).

## 2 EARTHQUAKE CATALOGUE

### 2.1 Catalogue compilation

The earthquake catalogue is primarily based on the published catalogue FCAT-17 (Manchuel et al., 2017). This catalogue includes historical events from France with location based on SISFRANCE (<http://www.sisfrance.net>) with re-evaluated moment magnitudes and hypocentral depths (see Manchuel et al. 2017). The instrumental period is equivalent to the SiHex catalogue (Cara et al., 2015). The geographical extension of FCAT-17 is limited to a 20 km buffer around the French borders and coastlines and we extended it by including the SiHex events located outside the buffer (original SiHex catalogue and extension provided by the authors upon request) as well as the SHEEC catalogue (developed within the SHARE project, Woessner et al., 2015), in order to cover a 200 km buffer around the French borders and coastlines. Both SiHex and SHEEC catalogue provide moment magnitude. We also included a temporal extension for the years 2010-2016 using the LDG bulletins (<http://www-dase.cea.fr>). The characteristics of the source catalogues are given in Table 1.

Table 1. Captions of tables; first letter capitalized, period at end, and centrally aligned.

Catalogue	Number of events	Time period	Magnitude range (M <sub>w</sub> )	Hypocentral depth range (km)
FCAT-17	41658	463-2009	0.4-6.7 (M <sub>w</sub> )	0-126
SHEEC	3003	1000-2006	1.7-6.6 (M <sub>w</sub> )	1-35
SiHex	38027	1962-2009	0.6-6.0 (M <sub>w</sub> )	0-126
SiHex extension	12581	1962-2009	0.9-5.6 (M <sub>w</sub> )	0-63
LDG bulletins	27038	2010-2016	0.2-5.4 (M <sub>L[LDG]</sub> )	0-77

### 2.2 Catalogue processing

We first identified duplicate events searching for events located less than 10 km away from each other and with an origin time difference less than 60 s. In a second step a manual review of these events allowed us to identify multiple entries in the catalogue.

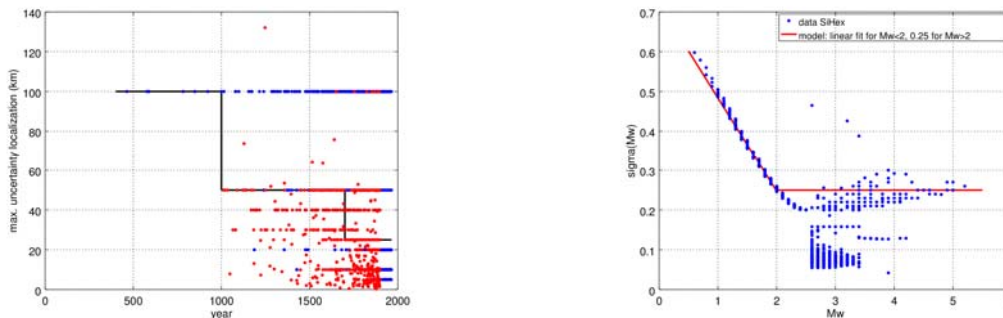


Figure 1. Time dependence of location uncertainty (left) (Blue dots: observed data from FACT-17; Red dots observed data from SHEEC; Black line: model derived from those data. Magnitude dependence of magnitude uncertainty (right). (Blue dots: observed data from SiHex; red line: model).

Location and magnitude uncertainty are not given for all the events of the catalogue. Since this information is used to compute Gutenberg-Richter models, we analyzed the reported location and magnitude uncertainties. In order to build simple models we analyzed variations with time and magnitude of the location and magnitude uncertainties. The analysis reveals that location uncertainty is primarily dependent on time while magnitude uncertainty is primarily dependent on magnitude. Figure 1 shows these dependencies and the models used in order to assign location and magnitude uncertainty to events for which those parameters are not reported.

For the period 2010-2016, the reported magnitude for the events is the local magnitude from the LDG. We first searched the moment tensor inversion databases of Bertrand Delouis (<https://geoazur.oca.eu/spip.php?rubrique59>) and of the Swiss Seismological Service. We identified about 50 events with a direct  $M_w$  estimation. For the other events we used the conversion scheme proposed by Cara et al. (2015) for the SiHex catalogue:

$$M_w = \begin{cases} 0.45 + 0.664 \times M_{L(LDG)} & \text{if } M_{L(LDG)} < 3.1 \\ M_{L(LDG)} - 0.6 & \text{if } M_{L(LDG)} \geq 3.1 \end{cases} \quad (1)$$

The final catalogue for the PSHA calculations includes finally 82778 events, covering the period 463-2016 with moment magnitudes between 0.5 and 6.7. It covers the region with latitudes between 39°N and 53.5°N and longitudes between 7°W and 11°E.

### 2.3 Completeness analysis

We performed a regional completeness analysis separating the offshore regions (Atlantic and Mediterranean), continental France, and mountainous regions. Intuitively, the potential to detect events in those regions is different. We also included a separate domain for the continental Europe outside France since the final catalogue for these areas is less robust than for continental France. Both the SHEEC and the SiHex catalogues which dominate these regions include less small events than the other catalogues.

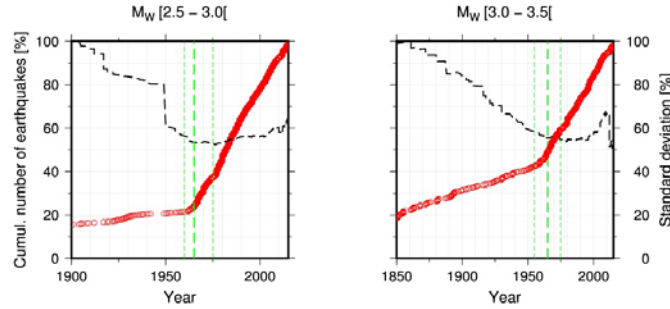


Figure 3. Examples of completeness analysis for the mountainous domain for the 2.5-3.0 (left) and the 3.0-3.5 (right) magnitude bins. The cumulative number of earthquakes is shown (red dots), as well as the standard deviation of the inter-event time (dashed black lines), and the completeness best estimate and upper and lower limits (dashed green lines).

To determine the periods of completeness we used the “slope method” based on the cumulative number of events along time, and the Hakimhashemi & Grünthal (2012) method based on the standard deviation of the inter-event time. The analysis is done for each domain and magnitude bins of 0.5 magnitude unit width (Figure 3). We looked for a break of slope in the cumulative number of events, together with a stable standard deviation of the inter-event time. We also imposed an increasing completeness with time. For each magnitude bin we determined a completeness best estimate as well as lower and upper bounds.

### 2.4 Declustering

We used the Gardner & Knopoff (1974) algorithm together with the space and time windows of Burkhard & Grünthal (2009). Note that the time windows are different for foreshocks and aftershocks. About half of the entries in the catalogue are identified as either aftershocks or foreshocks.

## 3 SSC MODEL

### 3.1 Area source models

Within regions of moderate seismic activity such as France, seismicity is usually diffuse and it is difficult to establish a relationship between epicenters and faults. Definition of seismic sources is based on regional subdivisions, covering areas of greater or lesser extent. The objective is to individualize crustal units of homogeneous seismogenic characteristics, following criteria related to static and dynamic state of the seismogenic crust (geometry and kinematic of tectonic structures, distribution of seismic activity, stress field...).

A seismotectonic analysis is conducted based on of geological, structural, geophysical, neotectonic and seismological data. This analysis allows the identification of the recent and existing deformation zones related to the current stress field, and to apprehend the deformation mechanisms associated with deep structures.

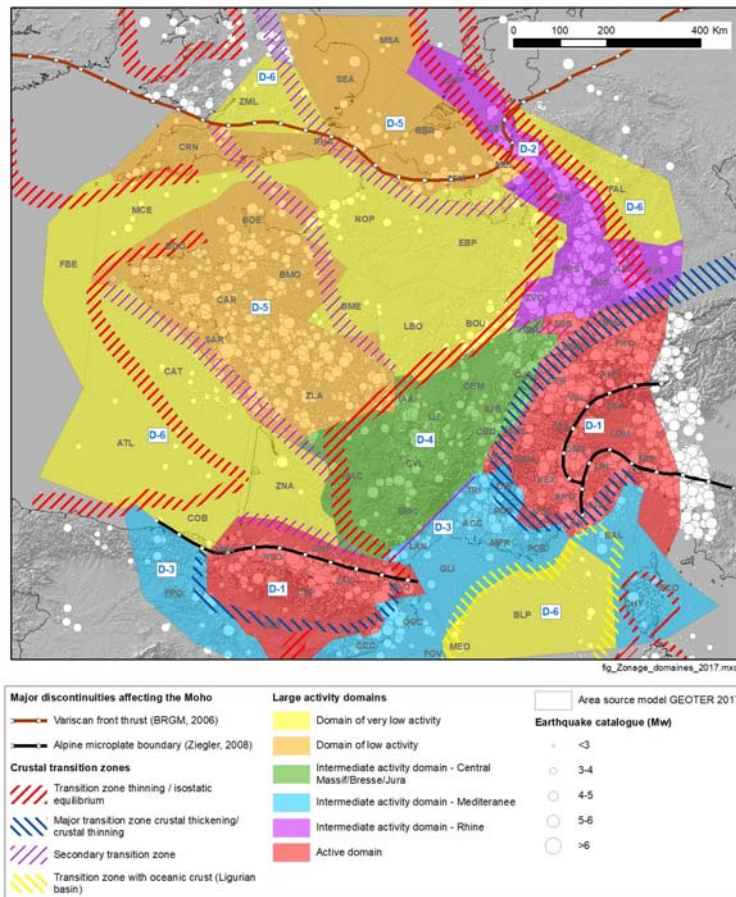


Figure 4. Area source model GTR 2017 and large activity domains.

The considered static and structural parameters are: (1) Moho isobaths, (2) gravimetric and magnetic data, (3) mapping of inherited structures (especially Variscan structures), (4) isopachs maps and Mesozoic sedimentary cover structuration within sedimentary basins, including the location of Triassic salt deposits, and (5) tertiary orogeny tectonic including Pyrenees, Alps and their surroundings.

The identification of seismotectonic units and definition of their boundary generally results from long discussions between specialists and draws from different disciplines to interpret the geological, seismological, geophysical and geodesic measurements and observations. This is why opinions may diverge on the definition of zones or the adoption of one or another model. In order to consider epistemic uncertainties related to the source zones delineation, it is common practice to consider several seismotectonic models in the logic tree. The epistemic uncertainty (i.e. the uncertainty associated with the modelling process) should be adequately assessed, to capture the full range of hypotheses regarding the characterization of the seismic sources and the frequencies of the earthquakes. For the present study, three area source models are considered:

- IRSN seismotectonic model published by Baize et al. (2013). Derived from the deterministic zonation published by Berge-Thierry et al. (2004), this model takes into account the most recent data regarding deep and shallow geology, as well as those related to tectonic and seismotectonic activity;
- GEOTER seismotectonic model which is regularly improved for PSHA studies in France by integration of the results of most recent research (Figure 4);
- EDF seismotectonic model (2017). This model corresponds to an update of the previous model developed as part of past seismic hazard assessments studies conducted for nuclear power plants by the EDF engineering centers.

### 3.2 Characterization of seismic activity

#### 3.2.1 Gutenberg-Richter models

The computation of seismic activity rates is based on the Gutenberg-Richter model which can be written as:

$$N = 10^{a-b \times M} \quad (2)$$

where N is the number of events with magnitude larger than or equal to M. Or in its truncated form:

$$N = 10^a \frac{e^{-b \times \ln(10) \times M} - e^{-b \times \ln(10) \times M_{\max}}}{1 - e^{-b \times \ln(10) \times M_{\max}}} \quad (3)$$

The method to determine the coefficients a and b of the model is based on the EPRI (2012) method which is an updated and improved version of the Weichert (1980) method. In particular, the method allows:

- The consideration of non-uniform magnitude bins;
- The use of regionally varying completeness periods;
- The introduction of a prior on the slope of the GR model (b-value);
- The propagation of uncertainties on earthquake location, magnitude and completeness periods through the use of synthetic catalogues.

A uniform distribution is used to propagate the uncertainty on completeness, while Gaussian distributions are used for location and magnitude uncertainty. The Gaussians are truncated at 3 sigmas for magnitude and 1 sigma for location uncertainty in order to avoid events occurring hundreds of kilometers away from their original locations.

Note that magnitude uncertainty can lead to bias in the estimation of the activity rates (Tinti & Mulargia, 1985; EPRI, 2012). Tinti & Mulargia, (1985) and EPRI (2012) proposed corrections of this bias based on adjustment of the computed recurrence rate by the exponential of the variance. The Tinti & Mulargia (1985) approach considers a constant magnitude uncertainty while the EPRI (2012) allows taking into account the specific uncertainty for each event of the catalog. EPRI (2012) also shows that this bias may potentially be inverted when the magnitudes included in the catalogue are not direct measures but converted from intensity or other magnitude scales. To solve this issue properly and apply a robust correction to the computed activity rates, the original direct measure and the eventual conversion scheme as well as associated uncertainties for each magnitude entry in the catalogue must be known. This has not been done in this study but will be considered in future updates.

The GR models are computed in two-steps. First we estimate a model for each of the six large domains defined at national level (Figure 4), using a prior on the b-value (slope of the GR model) equal to 1.0. These models are based on large catalogues (i.e. the domains cover wide geographical areas) and we expect stable estimates of the parameters a and b of the Gutenberg-Richter models. Then in a second step, GR models are computed for each area source using a prior value on the slope (b-value) equal to the b-value of the domain to which the zone belongs. Note that the correlation

between  $a$  and  $b$  is also computed. Figure 5 shows an example of GR fit to the domain D1 (high activity regions in France).

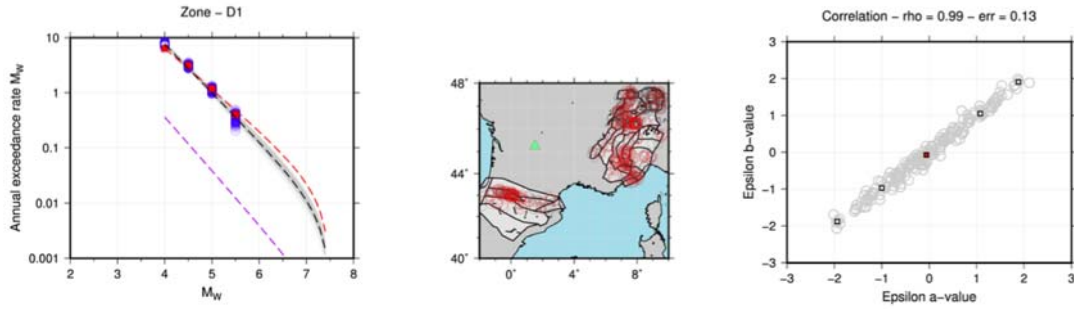


Figure 5. Summary plot of the GR analysis for domain D1. Seismic activity rates data and models are shown in the left panel (raw data: red squares; synthetic data after Monte Carlo: blue circles; raw GR model: dashed red line; individual fits and median of the GR using synthetic catalogues: grey and dashed black lines; reference level for SCR from Johnston et al., 1994: dashed purple line). The geographical extension of the area investigated and the earthquake catalogue are shown in the middle panel. The right panel shows the correlation between the  $a$ - and  $b$ -values (reduced centered variables).

### 3.2.2 Maximum magnitude

The definition of the maximum magnitude ( $M_{max}$ ) is based on a Bayesian approach (EPRI, 1994) considering large domain of recent deformation. The essence of the Bayesian approach is the development of a prior distribution of  $M_{max}$  based on the statistical analysis of a catalogue of earthquakes that occurred within tectonically analogous regions. The prior distribution is then updated using a likelihood function that is based on the number and size of earthquakes that occur within the seismic zone of interest. Several prior distributions for  $M_{max}$  are available (EPRI, 2012), including priors tailored for the application to the French context (Ameri et al., 2015).

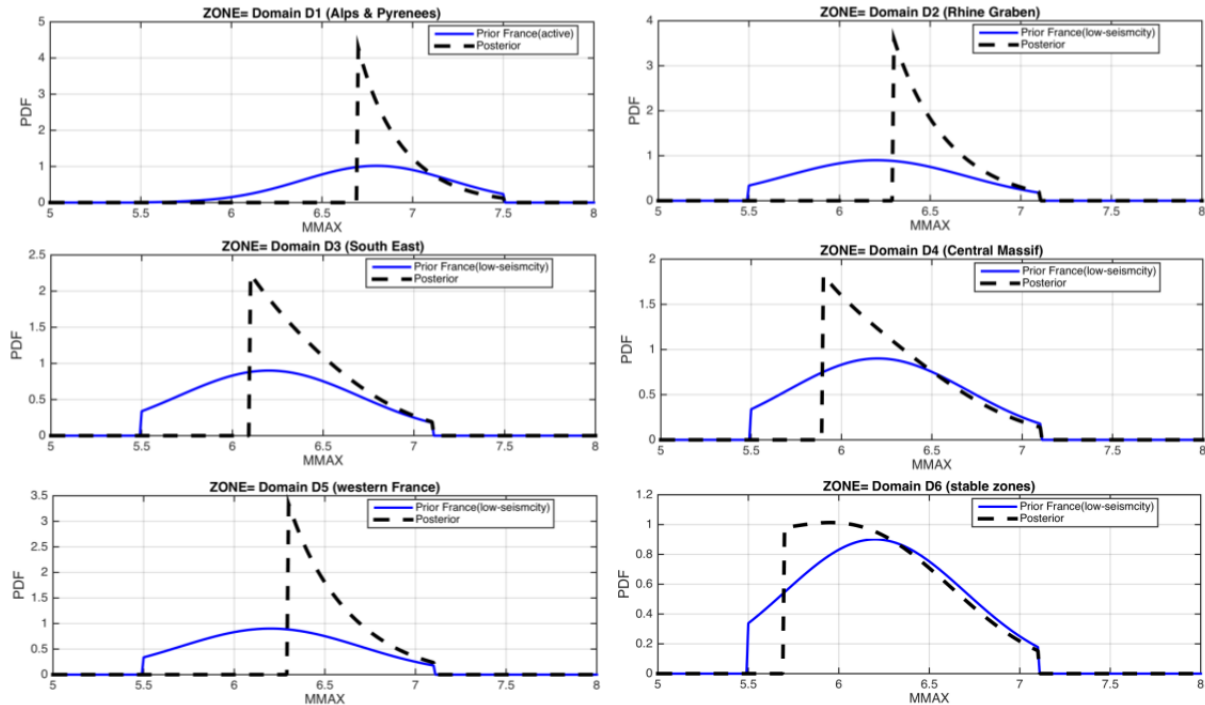


Figure 6. Maximum magnitude distributions (blue: prior; black: posterior) for the 6 large domains.

The method is applied to each large domain presented in Figure 4. The priors  $M_{max}$  distribution are truncated in the lower and upper tails as follows. The lower bounds of the prior  $M_{max}$  distributions are truncated at  $M_w=5.5$  for all domains because we consider that even in stable regions, we do not

have the appropriate data and geological arguments to exclude the occurrence of magnitude below Mw 5.5. The upper bounds are truncated at Mw=7.5 for the active domain and 7.1 for the others. The prior and posterior Mmax distributions are shown for each domain in Figure 6.

The choice of a single Mmax model is based on a sensitivity analysis that has been performed and showed little impact of the Mmax model on the hazard results at the targeted return periods (475 and 2475 years) .

### 3.3 Zoneless models

As an alternative to the area source models, the zoneless approach can be used to model seismic activity in the region of interest. The method relies on the seismic catalogue. For each event, a kernel function is used, which is a kind of spatial probability density function, and the summation of these kernels allows us to estimate the activity rates for a grid of points.

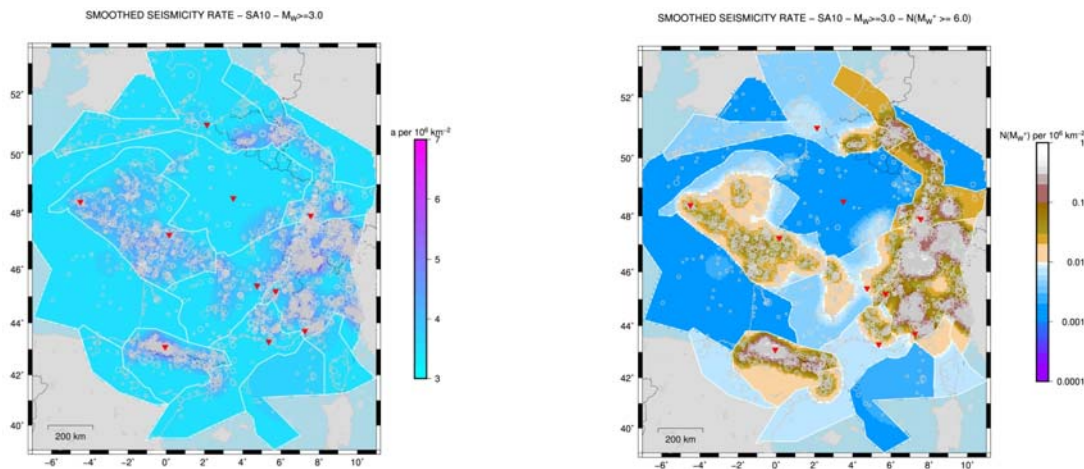


Figure 7. Map of the a-value per million squared kilometers computed with the zoneless model and a minimum magnitude of 3.0 (left). Map of the number of events of magnitude  $\geq 6.0$  per year computed using the zoneless model and a minimum magnitude of 3.0. The declustered catalogue filtered by completeness is also shown (grey circles), as well as the contours of the large seismotectonic domains (white lines).

A preliminary sensitivity analysis was carried on in order to test two algorithms to build the kernel functions, one called “adaptive” which uses the distance to a given number of closest events to define the kernel (Helmstetter & Werner, 2012), and another called “fixed” which defines a fixed kernel, the shape of which depends on magnitude only (similar to Woo, 1996 or Frankel, 1996). The sensitivity analysis showed that the parameterization of the kernels (number of closest events for the adaptive kernels or width of the kernel for the fixed ones) has little impact on the estimation of the activity rates. The minimum magnitude used to compute the kernels was also tested and the results also showed little impact. This led us to use a single smoothed seismicity model in the analysis.

The selected model is the adaptive kernel using the 10 closest events with a minimum magnitude of 3.0. The activity rates are estimated using a penalized maximum likelihood method using a prior b-value equal to those computed for the large seismotectonic domains. Note that strict boundary conditions are imposed meaning that the kernels cannot cross the domains boundaries. The regional completeness periods are also taken into account. Figure 7 shows the computed activity rates (a-values per million  $\text{km}^2$ ) and the map of the expected annual number of events with magnitude  $\geq 6.0$  predicted by the smoothed seismicity model. As a result of higher a-values and lower b-values in the most seismically active regions of France, the expected number of large magnitude events is much larger in those regions than in the more stable ones, which is clearly apparent in the figure.

We also compared the activity rates computed using the area source models and the zoneless approach. Figure 8 shows such a comparison for Grenoble.

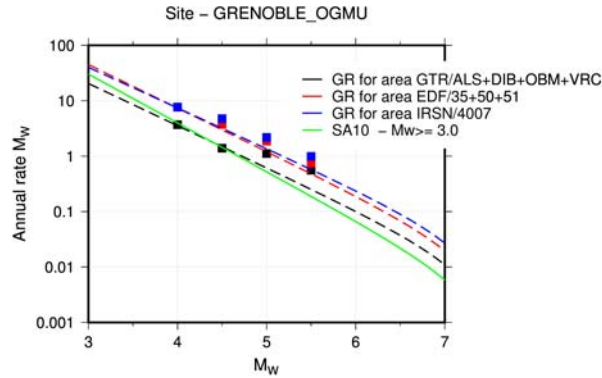


Figure 8. Comparison of the computed activity rates using the zoneless approach and the area source models for Grenoble (squares: observed activity rates using the different area source models; lines: seismic activity models).

## 4 GMC MODEL

### 4.1 Selection of GMPEs

The characterization of the ground motion in metropolitan France is clearly a major challenge. Metropolitan France is characterized by a low-to-moderate seismicity and consequently the available strong-motion records are very limited in the magnitude/distance range of interest for seismic hazard assessment. As a result, seismic hazard assessment in France is typically performed using GMPEs derived from data collected in other regions. A common approach to build a GMC model for PSHA (see Delavaud et al., 2012) consists in several steps:

- Pre-selection of GMPEs applicable for the target seismotectonic context;
- Critical review of the selected GMPEs through expert judgment (validity range of the modeling parameters, compatibility with the requirements of the PSHA calculation...);
- Comparison with observed strong-ground motion and ranking based on the results.

In this study, we made the assumption that GMPEs for active regions are the most relevant for the French context. We note, however, that in the SHARE project a mixture of GMPEs for active and stable regions have been used for central and western France. This approach would require adjustments between GMPEs especially in terms of site condition characteristics which would lead to an increase of the GMPEs standard deviations. Moreover, most of the GMPEs for SCR regions are developed for Eastern US which region is characterized by peculiar attenuation of ground-motion with distance (Bakun & McGarr, 2002).

Beauval et al. (2012) tested a number of these GMPEs against French strong-motion records and found that the best-fitting models over the whole frequency range are the Cauzzi and Faccioli (2008), Akkar and Bommer (2010), and Abrahamson and Silva (2008) models. However, these models are now superseded by more recent versions based on updated and augmented databases and functional forms.

Within the SIGMA project, a major outcome was the release of the RESORCE database (<http://www.resorce-portal.eu/>) that contains records for the Pan-European region, aiming at the testing and development of new GMPEs. Based on RESORCE, several new models have been produced (see Douglas et al., 2014). However, although being based on European data these GMPEs do not consider French records in their datasets. For this reason, two GMPEs have been developed focusing on the use of French data: the empirical model by Ameri (2014) and the stochastic model by Drouet and Cotton (2015).

The pre-selected models in the present study include the Pan-European models based on RESORCE, the NGA-West2 set of GMPEs (Bozorgnia et al., 2014) as well as the Cauzzi et al. (2015) and Drouet

& Cotton GMPEs. Based on the testing results by Beauval et al. (2012) and on our own critical review of the GMPEs, the final set of GMPEs is:

- Ameri (2014) (generic/RJB)
- Abrahamson et al., (2014)
- Cauzzi et al. (2015) (variable reference vS30 option)
- Drouet and Cotton (2015) (RRUP)

#### 4.2 Exploring proximity of GMPEs

The goal of the GMC logic tree is to capture the center, body and range of the technically defensible interpretations of ground motion models, representing the epistemic uncertainties in the GMC for the target site. Ideally these models would be mutually exclusive and collectively exhaustive (MECE). The challenge in building such a GMC logic tree is that many GMPEs could be proposed, but we are not sure that the selected models sample the ground-motion space adequately. For example, there may be redundant models; i.e. GMPEs that provide similar ground motions because they are based on the same data and models. These models artificially reduce the epistemic uncertainties. On the other hand, there may be missing models; i.e. models that are missing simply because we have not yet observed certain types of ground motions. In this framework, it is important to visualize the ground motions space that we would like our GMPEs set to cover.

We used several tools in order to explore the proximity of the selected GMPEs with respect to the full set of pre-selected GMPEs. We draw trellis plots to visualize the differences in distance and magnitude scaling, in spectral shapes and standard deviations. We also created Sammon's maps (see Scherbaum et al., 2010 for application of Sammon's maps to GMPEs visualization) which allow a visual comparison of ground-motions from various combinations of predictive parameters (M, R...) in single plots. Figure 9 presents an example of Sammon's map for 0.2 s spectral period showing that the selected GMPEs cover a large portion of the space delimited by the full set of pre-selected GMPEs. In addition, we also computed the hazard for a single SSC models using the selected GMPEs and the full set of GMPEs and compared the mean, maximum and minimum uniform hazard spectra (UHS) for both GMC models. All these tests allowed us to verify that the selected GMC model reasonably covers the center, body and range of the ground-motion distribution predicted by the full set of pre-selected GMPEs.

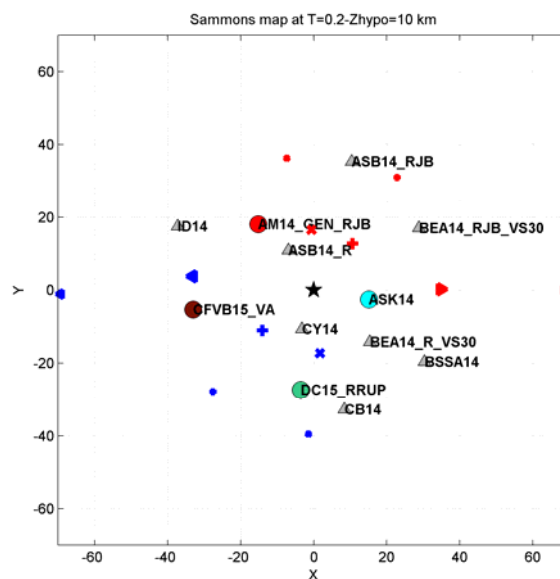


Figure 9. Sammon's map for 0.2 s spectral periods. Ground-motions predicted by the different GMPEs (grey triangles: all pre-selected GMPEs; colored circles: GMPEs selected for PSHA) have been computed for magnitudes between 4.5 and 6.5, and distances between 1 and 50 km (which are the scenarios that most contribute to hazard in low-to-moderate seismicity regions) and  $V_{S30}=800$  m/s. The black star represents the mean of all the GMPEs.

## 5 PSHA RESULTS

### 5.1 Logic-tree and Computation settings

The logic-tree used to compute PSHA includes 2 types of source models: 3 area sources and 1 zoneless model. The zoneless model is assigned a weight equal to 1/3 since at the target low return periods (475 and 2475 years) it is likely a good representation of future source distributions. The remaining 2/3 are equally distributed between the 3 area source models. The 4 GMPEs are equally weighted. We also propagated aleatory uncertainty related to depth distribution and virtual fault orientation. In addition, epistemic uncertainty on the seismic activity parameters and maximum magnitude is also propagated using Monte-Carlo sampling (100 samples). Gaussian distributions truncated at 3 sigmas are used for the seismic activity parameters and the distributions computed with the Bayesian method are used for Mmax.

The hazard is computed for 3 spectral periods PGA (100 Hz), 5 and 1 Hz. A grid of points with a mesh of 10 km is used. Standard rock site conditions with  $V_{S30}=800$  m/s are considered. Finally, the minimum magnitude considered in PSHA calculations is  $M_w=4.5$ . In order to run the PSHA calculations we used the Geoter in-house software SHAToolbox.

### 5.2 Seismic hazard maps

Figure 10 presents the hazard map computed for the mean PGA at 475 years return period. As expected the higher hazard is obtained in the Alps and the Pyrenees. The Paris and Aquitan Basins as well as most of central France present a low hazard level. The Armorican region to the West is characterized by an intermediate hazard level.

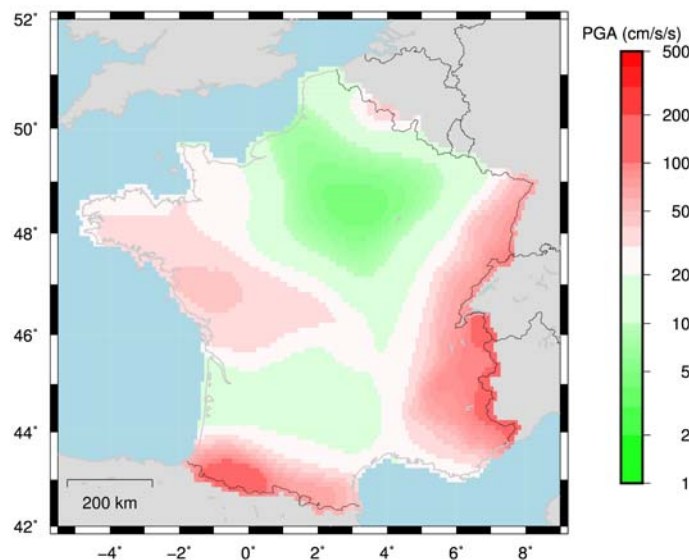


Figure 10. Hazard map for mean PGA at 475 years return period.

## 6 CONCLUSIONS

The probabilistic seismic hazard maps for the French territory presented in the present study aimed at integrating relevant scientific progress made in the last 15 years and in particular in the SIGMA project and compile the state of the art of PSHA in Europe and worldwide. The major scientific progress integrated were: the use of a new homogenous earthquake catalogue in  $M_w$  including instrumental and historical seismicity; the assessment of the maximum earthquake magnitude by applying a Bayesian approach adapted to the French context; the set of GMPEs used in the GMC logic tree was selected based on the most recent scientific progress; the SSC logic tree was improved by

considering recent progress in the PSHA practice and recent scientific publications.

The logic-tree includes 3 area source models as well as 1 zoneless model for the SSC, and 4 GMPEs for the GMC. Aleatory uncertainty on hypocentral depth and orientation of virtual faults are propagated in the hazard integral and epistemic uncertainty on seismic activity parameters and maximum magnitude is also included in the logic-tree. The seismic hazard maps are computed for the mean and median values at 3 spectral periods (1, 5 and 100 Hz) and 2 return periods (475 and 2475 years).

The results indicate that the hazard levels are lower than computed with the SHARE PSHA model (Woessner et al. 2015). The preliminary comparisons with recent PSHA models for Switzerland, Italy and Spain indicate a good agreement. Quantitative comparisons with these models are in progress.

The present study constitutes a first step of a long term project aiming at a continued improvement of the hazard model. In particular, sensitivity analysis on the application of the Bayesian updating methodology of the PSHA model have been performed, with the objective of updating the weights of the different branches of the logic-tree using a data-driven method. In parallel, the pseudo non-ergodic approach has been tested in order to assess its impact on hazard assessment at rock sites in France. As mentioned above, the seismic activity rates will also be reassessed trying to identify and correct any bias which may be linked with magnitude uncertainty.

## 7 ACKNOWLEDGMENTS

The authors would like to thank all of those who contributed significantly to the preparation of the paper. In particular, fruitful discussions with Emmanuel VIALLET, Christophe DUROUCHOUX, Paola TRAVERSA, and Pierre LABBE helped to improve the study.

## 8 REFERENCES

- Abrahamson N., Silva W.J. (2008). Summary of the Abrahamson & Silva NGA ground-motion relations, *Earthquake Spectra* 24, 67-97
- Abrahamson N. Silva W.J., Kamai R. (2014). Summary of the ASK14 Ground-Motion Relation for Active Crustal Regions. *Earthquake Spectra* 30 (3), p. 1025-1055
- Akkar, S., Bommer, J.J. (2010). Empirical equations for the prediction of pga, pgv and spectral accelerations in europe, the mediterranean region and the middle east. *Seismological research letters*, 81, 2, 195-206
- Ameri G. (2014). Empirical Ground Motion Model adapted to the French context. Deliverable SIGMA: SIGMA-2014-D2-131
- Ameri G., Baumont D., Gomes C., Le Dortz K., Le Goff B., Martin C., Secanell R. (2015). On the choice of maximum earthquake magnitude for seismic hazard assessment in metropolitan France – insight from the Bayesian approach. *9ème Colloque National AFPS 2015*, 30 novembre-2 décembre 2015, IFSTTAR.
- Baize S., Cushing E. M., Lemeille F. and Jomard H. (2013). Updated seismotectonic zoning scheme of Metropolitan France, with reference to geologic and seismotectonic data. *Bulletin de la Société Géologique de France* 184, n° 3, p. 225-259
- Bakun W. H., McGarr A. (2002). Differences in attenuation among the stable continental regions. *Geophysical Research Letters*, vol. 29, no. 23, 2121, doi:10.1029/2002GL015457.
- Beauval C., Tasan H., Laurendeau A., Delavaud E., Cotton F., Guéguen P., Kuehn N. (2012). On the testing of ground-motion prediction equations against small-magnitude data. *Bulletin of the Seismological Society of America*, 102 (5), 1994-2007
- Berge-Thierry C., Cushing E., Scotti O. and Bonilla F. (2004). Determination of the seismic input in France for the nuclear power plants safety : Regulatory context, hypothesis and uncertainties treatment. Proceedings of the CSNI Workshop on Seismic Input Motions, incorporating Recent Geological Studies, Tsukuba, Japan, 15-17 November, 14 p.

- Bozorgnia et al. (2014). NGA-West2 Research Project. *Earthquake Spectra*, Volume 30, No. 3, pages 973–987
- Burkhard, M., Grünthal, G. (2009). Seismic source zone characterization for the seismic hazard assessment project PEGASOS by the Expert Group 2 (EG 1b). - *Swiss Journal of Geosciences*, 102, 1, 149-188
- Cara, M., Cansi, Y., Schlupp, A. et al., 2015. SI-Hex: a new catalogue of instrumental seismicity for metropolitan France. *Bull. Soc. géol. France*, 2015, t. 186, no 1, pp. 3-19.
- Cauzzi C., Faccioli E. (2008). Broadband (0.05 to 20 s) prediction of displacement response spectra based on worldwide digital records. *Journal of Seismology*, Vol. 12, n° 4, p. 453-475
- Cauzzi C., Faccioli E., Vanini M., Bianchini A. (2015). Updated predictive equations for broadband (0.01 to 10 s) horizontal response spectra and peak ground motions, based on a global dataset of digital acceleration records. *Bulletin of Earthquake Engineering* 13 (6), p. 1587-1612
- Delavaud E., Cotton F., Akkar S., Scherbaum F., Danciu L., et al. (2012). Toward a Ground-Motion Logic Tree for Probabilistic Seismic Hazard Assessment in Europe. *Journal of Seismology* 16 (3), pp.451-473.
- Drouet, S., Cotton F. (2015). Regional Stochastic GMPEs in Low-Seismicity Areas: Scaling and Aleatory Variability Analysis—Application to the French Alps. *Bulletin of the Seismological Society of America* 105 (4), p. 1883-1902
- EPRI (1994), Johnston, A.C., Coppersmith K.J., Kanter L.R., Cornell C.A. (1994), The earthquakes of stable continental regions – Assessment of large earthquake potential. *Electric Power Research Institute (EPRI)*, TR-102261-V1, 2–1-98
- EPRI (2012). Technical Report: Central and Eastern United States Seismic Source Characterization for Nuclear Facilities. EPRI, Palo Alto, CA, U.S. DOE, and U.S. NRC: 2012.
- Frankel A. (1996). Mapping Seismic Hazard in the Central and Eastern United States. *Seismological Research Letters* 66 (4), p. 8-21.
- Gardner J. K. and Knopoff L. (1974). Is the sequence of earthquakes in southern California, with aftershocks removed, poissonian ?. *Bulletin of the Seismological Society of America*, Vol. 64, n° 5, p. 1363-1367
- Hakimhashemi A. H., Grünthal, G. (2012). A statistical method for estimating catalog completeness applicable to long-term nonstationary seismicity data. *Bulletin of the Seismological Society of America* 102(6), 2530-2546.
- Helmstetter A., Werner M. J. (2012). Adaptive Spatiotemporal Smoothing of Seismicity for Long-Term Earthquake Forecasts in California. *Bulletin of the Seismological Society of America*, Vol. 102, No. 6, pp. 2518–2529
- Manchuel K., Traversa P., Baumont D., Cara M., Nayman E., Durouchoux C. (2017). The historical and instrumental seismic catalogue for France (FCAT-17). *Bulletin of Earthquake Engineering*, 10.1007/s10518-017-0236-1.
- Martin, C., Ameri, G., Baumont, D., Carbon, D., Senfaute, G., Thiry, J. M., Faccioli, E., & Savy, J. (2017). Probabilistic seismic hazard assessment for southeastern France. *Bulletin of Earthquake Engineering*. DOI 10.1007/s10518-017-0249-9
- Pecker A, Faccioli E, Gurpinar A, Martin C, Renault P (2017) An overview of the SIGMA research project. Springer, Berlin. doi:10.1007/978-3-319-58154-5
- Scherbaum F. kuehn N. M., Ohrnberger M., Koehler A. (2010). Exploring the Proximity of Ground-Motion Models Using High-Dimensional Visualization Techniques. *Earthquake Spectra*, Volume 26, No. 4, pages 1117–1138
- Tinti S., Mulargia F. (1985). Effects of magnitude uncertainties on estimating the parameters in the Gutenberg-Richter frequency-magnitude law. *Bulletin of the Seismological Society of America* 75 (6): 1681–1697.
- Weichert D. H. (1980). Estimation of the earthquake recurrence parameters for unequal observation periods for different magnitudes. *Bulletin of the Seismological Society of America* 70 (4): 1337–1346.
- Woessner et al. (2015), The 2013 European Seismic Hazard Model: key components and results, *Bulletin of Earthquake Engineering*, 13, 12, pp 3553–3596
- Woo G. (1996). Kernel Estimation Methods for Seismic Hazard Area Source Modeling. *Bulletin of the Seismological Society of America*, Vol. 86, No. 2, pp. 353-362